

# Toxic Effects of Silver Ions on Early Developing Zebrafish Embryos Distinguished from Silver Nanoparticles

Martha S. Johnson, Preeyaporn Songkiatisak, Pavan Kumar Cherukuri, and Xiao-Hong Nancy Xu\*

Cite This: *ACS Omega* 2022, 7, 40446–40455

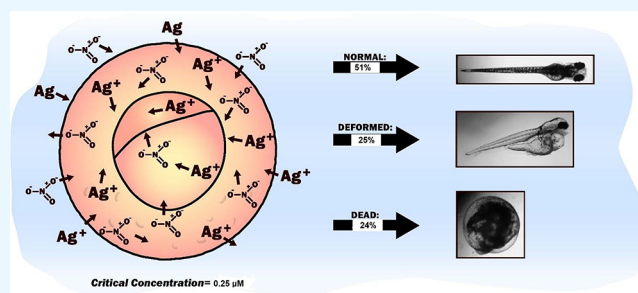
Read Online

ACCESS |

Metrics &amp; More

Article Recommendations

**ABSTRACT:** Currently, effects of nanomaterials and their ions, such as silver nanoparticles (Ag NPs) and silver ions ( $\text{Ag}^+$ ), on living organisms are not yet fully understood. One of the vital questions is whether nanomaterials have distinctive effects on living organisms from any other conventional chemicals (e.g., their ions), owing to their unique physicochemical properties. Due to various experimental protocols, studies of this crucial question have been inconclusive, which hinders rational design of effective regulatory guidelines for safely handling NPs. In this study, we chronically exposed early developing zebrafish embryos (cleavage-stage, 2 hours post-fertilization, hpf) to a dilution series of  $\text{Ag}^+$  (0–1.2  $\mu\text{M}$ ) in egg water (1 mM NaCl, solubility of  $\text{Ag}^+$  = 0.18  $\mu\text{M}$ ) until 120 hpf. We systematically investigated effects of  $\text{Ag}^+$  on developing embryos and compared them with our previous studies of effects of purified Ag NPs on developing embryos. We found the concentration- and time-dependent effects of  $\text{Ag}^+$  on embryonic development, and only half of the embryos developed normally after being exposed to 0.25  $\mu\text{M}$  (27  $\mu\text{g/L}$ )  $\text{Ag}^+$  until 120 hpf. As the  $\text{Ag}^+$  concentration increases, the number of embryos that developed normally decreases, while the number of embryos that became dead increases. The number of abnormally developing embryos increases as the  $\text{Ag}^+$  concentration increases from 0 to 0.3  $\mu\text{M}$  and then decreases as the concentration increases from 0.3 to 1.2  $\mu\text{M}$  because the number of embryos that became dead increases. The concentration-dependent phenotypes were observed, showing fin fold abnormality, tail and spinal cord flexure, and yolk sac edema at low  $\text{Ag}^+$  concentrations ( $\leq 0.2 \mu\text{M}$ ) and head and eye abnormalities along with fin fold abnormality, tail and spinal cord flexure, and yolk sac edema at high concentrations ( $\geq 0.3 \mu\text{M}$ ). Severities of phenotypes and the number of abnormally developing embryos were far less than those observed in Ag NPs. The results also show concentration-dependent effects on heart rates and hatching rates of developing embryos, attributing to the dose-dependent abnormally developing embryos. In summary, the results show that  $\text{Ag}^+$  and Ag NPs have distinctive toxic effects on early developing embryos, and toxic effects of  $\text{Ag}^+$  are far less severe than those of Ag NPs, which further demonstrates that the toxicity of Ag NPs toward embryonic development is attributed to the NPs themselves and their unique physicochemical properties but not the release of  $\text{Ag}^+$  from the Ag NPs.



## INTRODUCTION

Nanomaterials possess unique physicochemical properties that distinguish them from bulk materials and ions, owing to their small size and large surface area. It remains an open question about whether the effects of nanomaterials on living organisms and human health are unique or like either their bulk materials or ions.<sup>1–7</sup> Addressing this crucial question effectively would enable rational design of regulatory guidelines of nanomaterials for safe handling and manufacturing of nanomaterials and accelerating safe applications of nanomaterials and nanotechnology. Notably, toxic effects of heavy metals and their ions have been widely studied over decades. Therefore, transferring this knowledge to better understand nanotoxicity would accelerate the safe manufacturing of nanomaterials.

Silver metal, Ag NPs, and  $\text{Ag}^+$  possess distinctive physicochemical properties and have been used for a wide range of applications. For example, silver metal possesses the

highest conductivity and reflectivity of all metals and has been widely used in electronics, equipment, catalysis, traditional photography, jewelry, and foodware. Silver metal and ions exhibit antimicrobial effects and have been used in medicine.<sup>8–11</sup> Furthermore,  $\text{Ag}^+$  exhibit toxicity toward a wide range of living organisms, and EPA has set National Secondary Drinking Water Regulations (NSDWRs) that state a safe limit of  $\text{Ag}^+$  in drinking water at 0.10 mg/L.<sup>12</sup> Studies have shown that bare Ag NPs exhibit distinctive size-dependent

Received: August 26, 2022  
Accepted: October 10, 2022  
Published: October 26, 2022



localized surface plasmonic resonance (LSPR) optical properties<sup>13–15</sup> and dose-dependent antibacterial effects and toxicity toward living organisms.<sup>4–6,11,16–19</sup> Ag NPs have been increasingly used in consumer products (e.g., clothing and home appliances),<sup>20,21</sup> as well as in biomedical applications (e.g., antimicrobial agents, biosensors, and imaging probes).<sup>11,17,22–30</sup> We have found that low-dose Ag NPs and surface-modified Ag NPs are biocompatible, and they can be used as photostable imaging probes and single-molecule nanoparticle optical biosensors for real-time study of the signaling transduction pathway of single live cells, multidrug membrane transporters of single live cells, and embryonic nanoenvironments of developing zebrafish embryos.<sup>11,17,22–30</sup> We have also used Ag NPs as antibiotic drug nanocarriers to study the size-dependent inhibitory effect of drug nanocarriers against Gram-positive and Gram-negative bacteria.<sup>10,31,32</sup> Our studies have demonstrated that purified Ag NPs show dose-dependent and surface-dependent antibacterial effects by disrupting the cellular membrane and clogging the membrane transport.<sup>11,28</sup> Furthermore, we have systematically studied the dependence of effects of purified Ag and Au NPs on early developing zebrafish embryos on dose, size, surface charge, surface-modified molecules, and chemical properties of the purified NPs and developmental stages of zebrafish embryos.<sup>4–7,16,33–35</sup> Our studies show that the effects of the NPs on embryonic development highly depend upon the size, dose, chemical properties, surface charge, and modified molecules of the NPs, as well as developmental stages of embryos.<sup>4–7,16,33–35</sup>

Our previous studies show that the effects of the NPs on embryonic development were caused by Ag NPs but not Ag<sup>+</sup>.<sup>4–6,16,34,35</sup> Our NPs were purified, and we did not observe any substantial release of Ag<sup>+</sup> from Ag NPs during the exposure of embryos to Ag NPs. Nonetheless, a wide range of other studies reported conflicting findings. Many of these studies did not use purified Ag NPs and did not quantitatively characterize the concentration of Ag NPs and assumed that the toxicity of Ag NPs toward live cells and embryonic development was attributed to the release of Ag<sup>+</sup> from Ag NPs.<sup>21,36–38</sup> Residual of Ag<sup>+</sup> that were used to synthesize Ag NPs would be present in Ag NPs suspended in the solution. Therefore, it is crucial to wash and purify the NPs and collect the supernatant that resulted from washing NPs for control experiments, in order to study the distinctive effects of Ag NPs and Ag<sup>+</sup> on living organisms. Otherwise, the findings would be misleading. For example, some studies reported the observation of different toxicities of Ag NPs and Ag<sup>+</sup>.<sup>21,39–42</sup> However, many of these studies did not clearly describe the distinction of their effects quantitatively. Furthermore, many of these studies used either capped Ag NPs or unpurified Ag NPs.<sup>21,39–43</sup> Some of these studies investigated the effects of Ag NPs and Ag<sup>+</sup> on cultured cells, which could not offer the study of their effects on downstream signaling pathways and interactions of various cells in living organisms.

Unlike *in vitro* cultured cells, early developing zebrafish embryos offer the unique opportunity to study toxic effects of Ag NPs and Ag<sup>+</sup> on interactions and communications among all cell types in an intact living organism. Notably, differentiation of embryonic stem cells of early developing embryos is especially sensitive to toxic effects, which can serve as ultrasensitive *in vivo* assays to study toxicity of NPs and ions. Furthermore, early developing zebrafish embryos have distinctive advantageous over other *in vivo* model organisms

(e.g., mouse and rat).<sup>4,44–46</sup> For instance, zebrafish embryonic development exhibits well-defined developmental stages, and the embryos are translucent and develop outside their mothers, which enables real-time imaging of pathological and maldevelopment phenotypes *in vivo*.<sup>4,44–46</sup> Moreover, zebrafish (*Danio rerio*) share similar genetic phenotypes and drug binding sites as those in humans and have been used as *in vivo* model organisms for screening of efficacies of therapeutic agents and toxicities of conventional chemicals.<sup>47–50</sup> Massive amounts of zebrafish embryos can be generated rapidly at a very low cost, and zebrafish embryos fully develop rapidly within 120 hpf, enabling them to serve as ideal inexpensive *in vivo* assays to study biocompatibility, pharmacological efficacy, and toxicity of nanomaterials and ions. We have pioneered the use of early developing zebrafish embryos for the study of nanotoxicity and have used them as ultrasensitive *in vivo* assays to systematically study the dependence of effects of purified Ag and Au NPs on developing embryos on dose, size, surface charge, surface-modified molecules, and chemical properties of the purified NPs and developmental stages of zebrafish embryos.<sup>4–7,16,33–35</sup>

In this study, we used identical approaches to those used for the study of Ag NPs and quantitatively and systematically investigated the effects of Ag<sup>+</sup> on early developing zebrafish embryos by chronically exposing early developing zebrafish embryos (2 hpf, cleavage-stage embryos) to egg water (embryonic medium, 1 mM NaCl) containing a dilution series of Ag<sup>+</sup> concentrations (0, 0.05, 0.1, 0.2, 0.3, 0.4, 0.8, and 1.2  $\mu$ M), instead of Ag NPs. We then compared the concentration-dependent toxicity of Ag<sup>+</sup> on embryonic development with those of Ag NPs using their critical concentration at which only half of the embryos developed normally and concentration-dependent developmental phenotypes, aiming to determine their distinctive effects on embryonic development. We also studied the concentration-dependent heart rate and hatching time of normally developing and abnormally developing embryos that were chronically exposed to Ag<sup>+</sup> over 120 hpf, aiming to understand their underlying mechanisms.

## ■ MATERIALS AND METHODS

**Reagents and Supplies.** Deionized (DI) water (18 M $\Omega$ , Barnstead) was used to prepare all solutions. Silver nitrate (AgNO<sub>3</sub>, >99%, SigmaUltra) was purchased from Sigma. Stock solutions of AgNO<sub>3</sub> in DI water were prepared and stored in the dark at 4 °C until they were used.

**Breeding and Monitoring of Zebrafish Embryos.** Wild-type adult zebrafish were housed in a stand-alone system (Aquatic Habitats), and they were maintained and bred, as we reported previously.<sup>4–7,16,33–35</sup> Specifically, we placed four female adult zebrafish with three male adult zebrafish in a 10.0 L breeding tank (Pentair Aquatic Habitats) containing the fresh circulated system water and maintained it at 28.5 °C around 7 PM. A light (14 h) and dark (10 h) cycle was used to trigger breeding and fertilization of embryos. Once the light was on the next morning, eggs were laid and fertilized. Healthy fertilized embryos were collected and placed in the fresh system water using a siphoning collection hose, then transferred into a Petri dish containing egg water (1.0 mM NaCl), and washed three times with egg water to remove the surrounding debris. The healthy embryos were imaged, selected, and used for the experiments. All experiments involving embryos and zebrafish were conducted using the

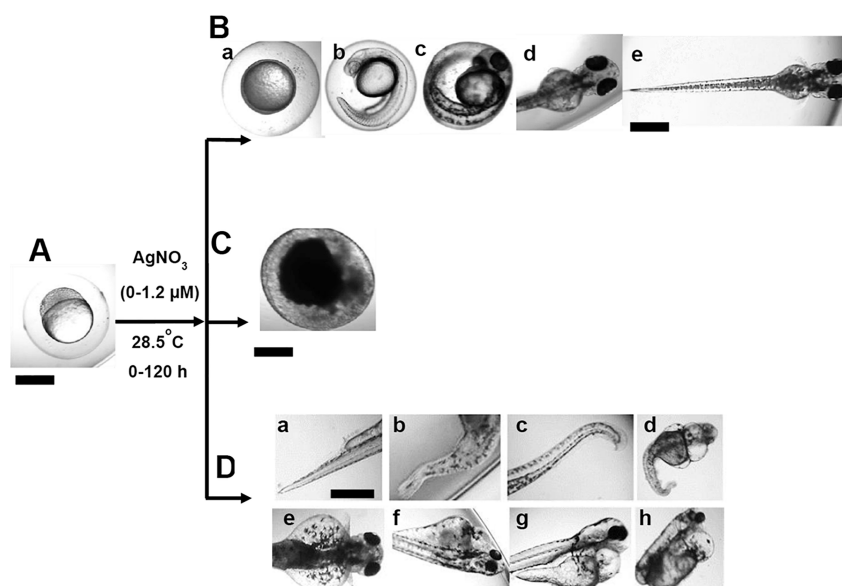


**Figure 1.** Experimental design for the study of concentration- and time-dependent toxic effects of  $\text{Ag}^+$  on embryonic development of zebrafish: (A) cleavage-stage embryos (2 hpf) were exposed to various concentrations (0–1.20  $\mu\text{M}$ ) of  $\text{AgNO}_3$  over 120 h at 28.5 °C and imaged every 24 h. (B) Representative developmental stages of normally developing embryos: (a) germ-ring stage (8–10 hpf), (b) late segmentation stage (24 hpf), (c) hatching stage (48 hpf), (d) protruding mouth pharyngula stage (72 hpf), and (e) fully developed larvae's (120 hpf) lateral view. (C) Dead embryos. (D) Abnormally developed zebrafish larvae at 120 hpf show (a–d) fin fold abnormality, (b–d) tail/spinal cord flexure and truncation, (e–g) pericardial sac edema and yolk sac edema, and (h) eye and head abnormalities and pericardial sac edema and yolk sac edema. The larvae with eye and head developmental abnormalities are often accompanied with multiple types of other deformities. Scale bar for (A–D) = 500  $\mu\text{m}$ .

approved protocols (protocol no. 15-012) in compliance with Institutional Animal Care and Use Committee (IACUC) guidelines.

**Study of Concentration-Dependent Toxicity of  $\text{Ag}^+$  on Embryonic Development.** Once embryos reached the cleavage stage ( $\sim 2$  hpf), embryos were incubated with egg water (1.0 mM NaCl) containing a dilution series of  $\text{AgNO}_3$  (0.00, 0.05, 0.10, 0.20, 0.30, 0.40, 0.80, and 1.20  $\mu\text{M}$  or 0, 5.4, 10.8, 21.6, 32.4, 43.2, 86.4, and 129.6  $\mu\text{g/L}$ ) in 24-well plates with one embryo per well containing a 2 mL solution for 120 h, as shown in Figure 1. The plates were incubated in a water bath at 28.5 °C for 120 h under dark conditions to prevent the photoreaction of  $\text{Ag}^+$ . The developing embryos were imaged and recorded to observe their development, heartbeats, hatching, and phenotypes, over time at 2, 4, 24, 48, 72, 96, and 120 hpf using bright-field optical microscopy (an inverted microscope, Zeiss Axiovert) equipped with a CCD camera (Coolsnap, Roper Scientific) and a color camcorder (Sony). Twelve embryos with one embryo per well for each given concentration of  $\text{Ag}^+$  were studied individually as one trial. Three replicates with the total number of 36 embryos with one embryo in an independent well containing each given concentration of  $\text{Ag}^+$  were studied individually.

**Quantitative Study of Concentration-Dependent Effects of  $\text{Ag}^+$  on the Heartbeat of Developing Embryos and Larvae.** Videos of heartbeats of developing embryos exposed to the given concentrations of  $\text{AgNO}_3$  (0.00, 0.05, 0.10, 0.20, 0.30, 0.40, 0.80, and 1.20  $\mu\text{M}$ ) at 24, 48, and 120 hpf were acquired in real time using a digital camcorder (Sony) and a CCD camera (Coolsnap Ez, Roper Scientific) with 100 frames per second over time. The videos were analyzed to determine the heart's contractions and heartbeat per minute (BPM) for each embryo at each given time.

**Study of Concentration-Dependent Effects of  $\text{Ag}^+$  on the Hatching Rate of Developing Embryos.** Videos and

images of developing embryos exposed to the given concentrations of  $\text{AgNO}_3$  (0.00, 0.05, 0.10, 0.20, 0.30, 0.40, 0.80, and 1.20  $\mu\text{M}$ ) around hatching stages (46–96 hpf) were acquired in real time every 2 h until 120 hpf using a digital camcorder (Sony) and a CCD camera (Coolsnap Ez, Roper Scientific), to determine newly hatched larvae emerging from the embryonic barrier of the chorions. Abnormalities of hatched larvae were also thoroughly imaged, recorded, and analyzed. The hatching rates at each 10 h duration, 46–56, 57–66, 67–76, 77–86, and 87–96 hpf, were determined by dividing the number of newly hatched embryos at each given 10 h duration by the total number of developing embryos incubated with the given concentration of  $\text{Ag}^+$ .

**Data Analysis and Statistics.** For each trial, a minimum of 12 embryos (each embryo in a well) were exposed to each given concentration of  $\text{AgNO}_3$  individually. Each experiment was performed at least three times. Therefore, a minimum of 36 embryos exposed to each given concentration of  $\text{Ag}^+$  (each embryo treated with the concentration in a well individually) were studied to gain sufficient data for statistical analysis, permitting the study of the effects of  $\text{Ag}^+$  on a large population of embryos at the single-embryo resolution. The mean of three measurements (12 embryos for each concentration and each trial) with a standard deviation of the number of normally developing, abnormally developing, and dead embryos versus the concentration of  $\text{Ag}^+$  over time is used to study  $\text{Ag}^+$  concentration-dependent and exposure time-dependent effects of  $\text{Ag}^+$  on the embryonic development (Figure 2). The overall distribution of phenotypes of abnormally developed embryos from all three measurements (36 embryos) over the concentration of  $\text{Ag}^+$  is presented in Figure 3. We use the mean of three measurements (12 embryos for each concentration and each measurement) with a standard deviation of the heartbeat ( $\text{min}^{-1}$ ) of normally developing and abnormally developing embryos versus the concentration



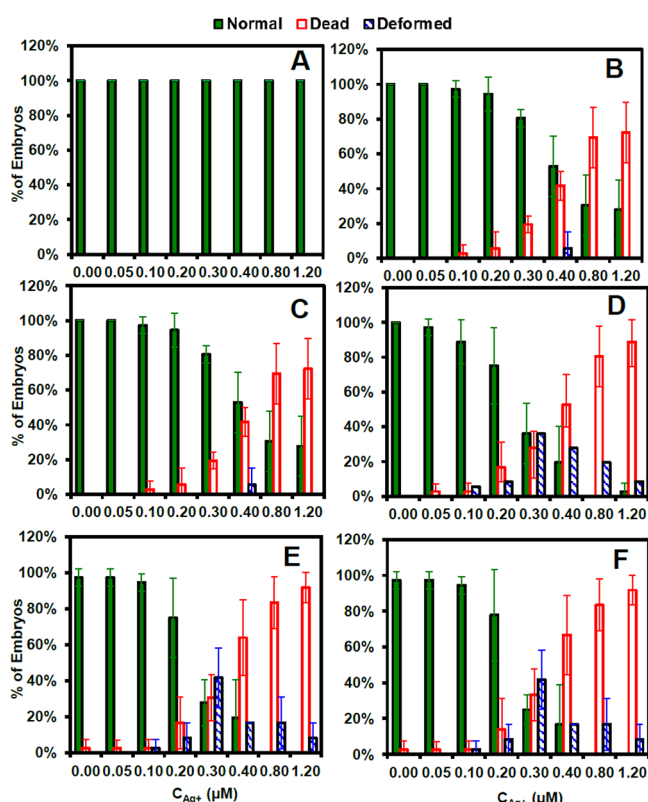
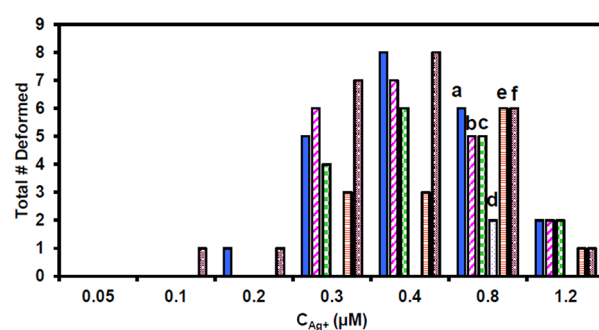


**Figure 2.** Concentration- and time-dependent toxic effects of  $\text{Ag}^+$  on embryonic development of zebrafish. Histograms of the percentage of embryos that developed normally (green), abnormally (blue), or became dead (red) versus the concentration of  $\text{Ag}^+$  for cleavage-stage embryos (2 hpf) that were chronically exposed to each given concentration of  $\text{Ag}^+$  until (A) 4, (B) 24, (C) 48, (D) 72, (E) 96, and (F) 120 hpf show that the toxic effects of  $\text{Ag}^+$  on embryonic development highly depend on the concentration of  $\text{Ag}^+$  and exposure time. As the  $\text{Ag}^+$  concentration increases and as the exposure time increases, the number of embryos that developed normally decreases. Only half of the embryos developed normally at 120 hpf in the presence of  $0.25 \mu\text{M}$   $\text{Ag}^+$  (a critical concentration). Abnormalities of developing embryos (24–120 hpf) were determined and characterized by comparing them with respective developmental stages of normally developing embryos in the absence of  $\text{Ag}^+$  (control experiments). The developing embryos were followed closely throughout the entire duration of the experiment over 120 h, and their phenotypes were scored and classified as summarized in Table 1.

of  $\text{Ag}^+$  at 24, 48, and 120 hpf to study dose-dependent effects of  $\text{Ag}^+$  on the heartbeat of developing embryos (Figure 4). The overall distribution of the percent of hatched embryos from all three measurements over the concentration of  $\text{Ag}^+$  over time is presented in Figure 5. Conventional statistical analysis methods (*t*-test, ANOVA, Tukey's, SigmaStat 3.5 with  $P = 0.05$ ) were used to determine the significance of the different observations among all concentrations (Figures 2 and 4). A pairwise *t*-test comparison was performed to evaluate the distribution of deformities over the concentration of  $\text{Ag}^+$  in Figure 3.

## RESULTS AND DISCUSSION

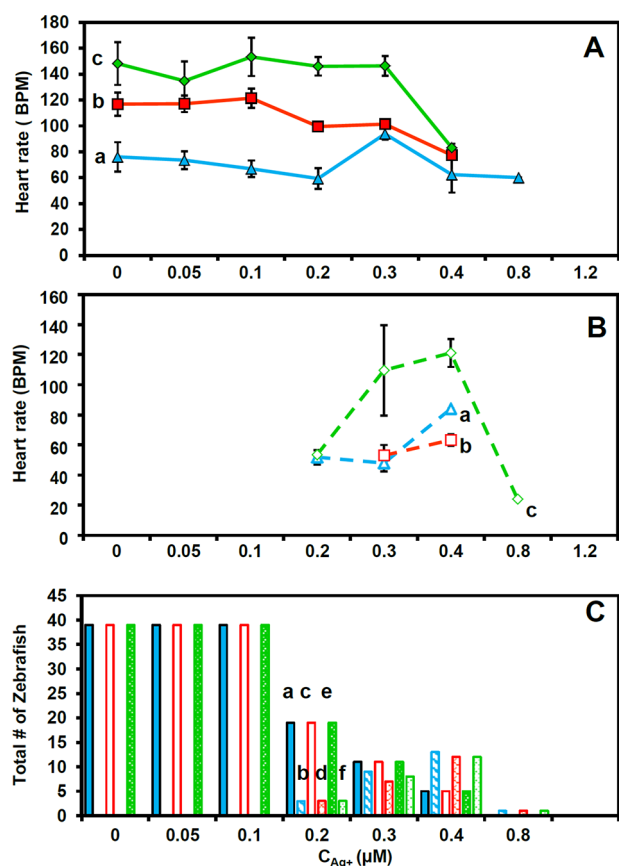
**Study of Concentration- and Time-Dependent Effects of  $\text{Ag}^+$  on Embryonic Development.** To study the concentration-dependent effect of  $\text{Ag}^+$  on embryonic development, we chronically incubated cleavage-stage zebrafish



**Figure 3.** Histogram of distribution of the number of deformed larvae with a given phenotype developed from the cleavage-stage embryos that were chronically exposed to a given concentration of  $\text{Ag}^+$  until 120 hpf: (a) fin fold abnormality (blue-colored bars), (b) tail flexure (pink diagonal-filled bars), (c) yolk sac edema (green checkerboard-filled bars), (d) eye abnormality (lightly violet dot-filled bars), (e) head abnormality (horizontal red line-filled bars), and (f) pericardial sac edema (heavily dot-filled brown bars), showing the high dependence of phenotypes on the concentration of  $\text{Ag}^+$ . The accumulative number of larvae with each given phenotype from all three trials is presented. Note that each larva with multiple phenotypes was counted multiple times based upon each phenotype.

embryos ( $\sim 2$  hpf) in egg water (embryonic medium, 1 mM NaCl) containing a dilution series of  $\text{AgNO}_3$  (0– $1.20 \mu\text{M}$ ) at  $28.5^\circ\text{C}$  over 120 h and imaged vital embryonic developmental stages at 4, 24, 48, 72, 96, and 120 hpf (Figure 1 and Table 1). The number of normally developing embryos, abnormally developing embryos with specific phenotypes, and dead embryos were recorded and plotted against the concentration of  $\text{Ag}^+$  at each respective developmental stage (Figure 2). The results show that all embryos incubated with egg water containing  $\text{Ag}^+$  (0– $1.2 \mu\text{M}$ ) were alive and developed normally at 4 hpf (Figure 2A). As the exposure time of developing embryos to  $\text{Ag}^+$  increases to 24 hpf (Figure 2B), as the  $\text{Ag}^+$  concentration increases, the number of normally developing embryos decreases from 100% at  $0.05 \mu\text{M}$  to 81% at  $0.30 \mu\text{M}$  and 28% at  $1.20 \mu\text{M}$ , while the number of dead embryos increases from 3% at  $0.10 \mu\text{M}$  to 72% at  $1.2 \mu\text{M}$ , and abnormally developing embryos (6%) were observed only at  $0.4 \mu\text{M}$  (Figure 2B). Similar results were observed at 48 hpf (Figure 2C).

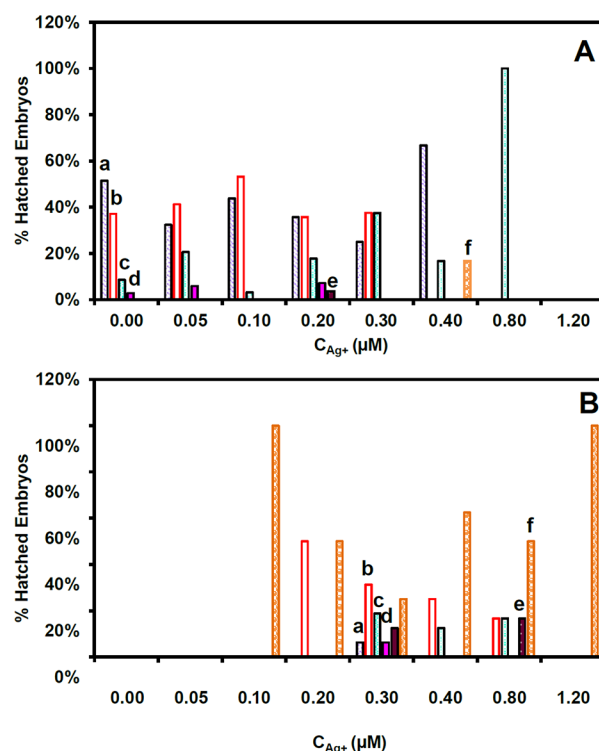
As the exposure time of developing embryos to  $\text{Ag}^+$  increases to 72 hpf (Figure 2D), as the  $\text{Ag}^+$  concentration increases, the number of normally developing embryos decreases drastically from 97% at  $0.05 \mu\text{M}$  to 36% at  $0.30 \mu\text{M}$  and 3% at  $1.20 \mu\text{M}$ , while the number of dead embryos increases rapidly from 3% at  $0.05 \mu\text{M}$  to 89% at  $1.2 \mu\text{M}$ . Interestingly, a considerable number of abnormally developing embryos were observed, which increases with the  $\text{Ag}^+$  concentration from 6% at  $0.10 \mu\text{M}$ , 8% at  $0.20 \mu\text{M}$ , and 36% at  $0.3 \mu\text{M}$ , and then decreases as the  $\text{Ag}^+$  concentration increases to 28% at  $0.40 \mu\text{M}$ , 19% at  $0.80 \mu\text{M}$ , and 8% at  $1.2 \mu\text{M}$ , attributing to the increase of dead embryos as the  $\text{Ag}^+$  concentration reaches  $0.3 \mu\text{M}$  and beyond. As the exposure time of developing embryos to  $\text{Ag}^+$  increases further to 96 hpf (Figure 2E), similar trends were observed. The number of normally developing embryos decreases further from 97% at  $0.05 \mu\text{M}$  to 28% at  $0.30 \mu\text{M}$ , and none of embryos developed normally at  $0.80 \mu\text{M}$  or higher concentrations, while the number of dead embryos increases from 3% at  $0.05 \mu\text{M}$  to 92% at  $1.2 \mu\text{M}$ . The number of abnormally developing embryos



**Figure 4.** Concentration- and time-dependent effects of  $\text{Ag}^+$  on heart rates of developing embryos treated chronically with  $\text{Ag}^+$  from the cleavage stage (2 hpf) until 120 hpf. (A) Plot of the heart rate of normally developing embryos versus the concentration of  $\text{Ag}^+$  at (a) 24 (solid triangles), (b) 48 (solid squares), and (c) 120 hpf (solid diamonds). (B) Plot of the heart rate of abnormally developing embryos versus the concentration of  $\text{Ag}^+$  at (a) 24 (triangles), (b) 48 (squares), and (c) 120 hpf (diamonds). (C) Total number of developing embryos used for measuring the heart rates at the given concentration and given time point in (A,B): (a) normally developing embryos at 24 hpf (solid cyan bars), (b) abnormally developing embryos at 24 hpf (cyan diagonal-filled bars), (c) normally developing embryos at 48 hpf (red empty bars), (d) abnormally developing embryos at 48 hpf (red-patterned bars), (e) normally developed larvae at 120 hpf (green-filled white-dotted bars), and (f) abnormally developed larvae at 120 hpf (green-dotted bars).

increases with the  $\text{Ag}^+$  concentration from 3% at 0.10  $\mu\text{M}$  to 8% at 0.20  $\mu\text{M}$  and 42% at 0.30  $\mu\text{M}$  and then decreases as the  $\text{Ag}^+$  concentration increases to 17% at 0.40  $\mu\text{M}$  and 8% at 1.2  $\mu\text{M}$ , owing to the increase of dead embryos at the higher concentration (>0.30  $\mu\text{M}$ ). As the exposure time of developing embryos to  $\text{Ag}^+$  increases further to 120 hpf (Figure 2F), concentration-dependent toxic effects of  $\text{Ag}^+$  on embryonic development are similar to those observed at 96 hpf (Figure 2E).

Taken together, the results in Figure 2 show the significant concentration-dependent and time-dependent toxic effects of  $\text{Ag}^+$  on embryonic development, indicating the critical concentration of 0.25  $\mu\text{M}$  at which only 51% of chronically treated cleavage-stage embryos developed normally at 120 hpf. Significant toxic effects of  $\text{Ag}^+$  on embryonic development were observed as early as 24 hpf (22 h incubation) and reached the maximum effects at 72 hpf (70 h incubation) and remained

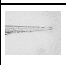






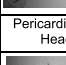


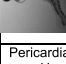
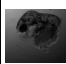
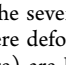



**Figure 5.** Concentration-dependent effects of  $\text{Ag}^+$  on hatching rates of developing embryos treated chronically with  $\text{Ag}^+$  from the cleavage stage (2 hpf) until 120 hpf. Histogram of the percentages of developing embryos that successfully hatched during exposure to each given concentration of  $\text{Ag}^+$ . (A) Normally developed and (B) abnormally developed larvae hatched during (a) 46–56 (violet diagonal-filled bars), (b) 57–66 (red empty bars), (c) 67–76 (cyan-patterned bars), (d) 77–86 (solid pink bars), and (e) 87–96 hpf (maroon-filled white-dotted bars) and (f) unhatched at 120 hpf (orange-ball-filled bars). The hatching of embryos was imaged and recorded every 2 h during their exposure to the given concentration of  $\text{Ag}^+$ . The percentage of embryos that hatched during each given period versus the concentration of  $\text{Ag}^+$  is calculated by dividing the hatched embryos by the total number of embryos at each given concentration, and it is presented cumulatively from all three measurements.

nearly plateaued after that. The results demonstrate that the early developing embryos are more sensitive to the effects of  $\text{Ag}^+$ , suggesting that fully developed larvae are more resilient against toxic effects of  $\text{Ag}^+$  than early developing embryos.

The histogram of the number of abnormally developed embryos with specific phenotypes at 120 hpf versus the concentration of  $\text{Ag}^+$  in Figure 3 and Table 1 shows that developmental phenotypes highly depend upon the concentration of  $\text{Ag}^+$ . At the lower concentration (0.1  $\mu\text{M}$ ), only one abnormally developed larva with fin fold abnormalities, tail and spinal cord flexure and truncation, and pericardial sac edema and yolk sac edema was observed. As the concentration increases to 0.2  $\mu\text{M}$  and higher, additional phenotypes of head and eye abnormalities were observed, and the severity of abnormalities also increases, as summarized in Table 1. We ranked the severity of developmental phenotypes based upon the morphological deviations from the normally developed larvae using a scoring system that we developed for the study of effects of  $\text{Ag}$  NPs on embryonic development.<sup>4–7,16,33–35</sup> For example, we semiquantitatively assigned the scale deformity from 0 (normal) to 4 (the severest) to rank the

Table 1. Summary of Concentration-Dependent Toxicity of Ag<sup>+</sup> on Embryonic Development<sup>a</sup>

C <sub>Ag+</sub> (μM)	Images of Zebrafish	Number of zebrafish with Severity Scale <sup>1</sup>					Number of Dead Embryos
		0	1	2	3	4	
0	Normal Development	35					1
							
0.1	Fin fold Abnormalities	34			1*		1
							
	Tail & Spinal Cord Flexures and Truncations				1*		
							
0.2	Pericardial Sac Edema & Yolk Sac Edema				1*		
							
0.3	Fin fold Abnormalities	28		2*	1*		5
							
	Tail & Spinal Cord Flexures and Truncations				1*		
							
0.4	Pericardial Sac Edema, Yolk Sac Edema, Head and Eye Abnormalities					1*	5*
							
	Fin fold Abnormalities	0				6*	30
							
0.8	Tail & Spinal Cord Flexures and Truncations					5*	
							
	Pericardial Sac Edema, Yolk Sac Edema, Head and Eye Abnormalities						6*
							
1.2	Fin fold Abnormalities	0				2*	33
							
	Tail & Spinal Cord Flexures and Truncations					1*	2*
							
1.2	Pericardial Sac Edema, Yolk Sac Edema, Head and Eye Abnormalities					1*	2*
							

<sup>a</sup>The severities of phenotypes of developed zebrafish larvae are scored using the scale of 1 as the least severe deformed larvae and 4 as the most severe deformity, and zero is the normally developed zebrafish larvae. \*Those severely deformed larvae with multiple types of deformities (two or more) are listed in multiple categories and scored higher and marked with an asterisk (\*). Scale bar = 500 μm for all images.

severities of fin fold abnormality, tail and spinal cord flexure and truncation, pericardial sac edema and yolk sac edema, and head and eye abnormality, respectively. The larvae with a high degree of eye and head abnormalities were often accompanied with other abnormalities (e.g., fin fold abnormality, tail and spinal cord flexure and truncation, and pericardial sac edema and yolk sac edema), suggesting that the interconnectivity of developmental pathways and downstream pathways of head development could potentially lead to other deformities.

**Study of Concentration-Dependent and Time-Dependent Effects of Ag<sup>+</sup> on Heartbeats of Developing Embryos.** The heartbeats of normally developing embryos at 24, 48, and 120 hpf were measured and plotted against the Ag<sup>+</sup> concentration in Figure 4A, showing that the heartbeats of normally developing embryos at 24, 48, and 120 hpf in the absence of Ag<sup>+</sup> are 76 ± 11, 117 ± 9, and 148 ± 16 beats per min (BPM), respectively. The result demonstrates that the heartbeats of normally developing embryos increase as the 24 hpf embryos develop to the 120 hpf larvae. As the concentration of Ag<sup>+</sup> increases from 0 to 0.1 μM, the heartbeats of normally developing embryos at 24, 48, and

120 hpf remain essentially unchanged. As the concentration increases further from 0.1 to 0.8 μM, the heartbeats of normally developing 24 hpf embryos remain essentially unchanged. Interestingly, as the concentration increases from 0.05 to 0.4 μM, the heartbeats of normally developing 48 hpf embryos gradually decrease from 121 ± 8 to 77 BPM. Notably, as the concentration increases from 0.05 to 0.3 μM, the heartbeats of normally developed 120 hpf larvae remain essentially unchanged. As the concentration increases further from 0.3 to 0.4 μM, the heartbeats of 120 hpf larvae decrease sharply to 83 ± 3 BPM. As the concentration of Ag<sup>+</sup> increases to 0.8 μM and higher, only abnormally developed 48 and 120 hpf larvae were observed. The results in Figure 4A show that effects of Ag<sup>+</sup> on the heartbeats of developing embryos highly depend upon the concentration, exposure time, and developmental stage. At 24 hpf, the heart was being developed and the heartbeat just started, and the developing embryos were exposed to Ag<sup>+</sup> only for 22 h. Thus, the concentration-dependent effects of Ag<sup>+</sup> on heartbeats of 24 hpf developing embryos are less pronounced. As the exposure time increases, the concentration-dependent effects of Ag<sup>+</sup> on heartbeats of 48



hpf developing embryos become more pronounced, while the effects of  $\text{Ag}^+$  on the heartbeats of normally developed 120 hpf larvae become even more striking as the concentration increases from 0.3 to 0.4  $\mu\text{M}$ .

The heartbeats of abnormally developing embryos at 24, 48, and 120 hpf are considerably lower than those of normally developing embryos at the respective developmental stage, correspondingly. The heartbeats of abnormally developing embryos are highly associated with phenotypes, and they vary substantially. In general, the 120 hpf deformed larvae still show faster heartbeats than 24 and 48 hpf abnormally developing embryos. However, for the severely deformed larvae at 120 hpf, the heartbeats could be as slow as 24 BPM. Taken together, the results in Figure 4 show that the heartbeats of the developing embryos and larvae highly depend upon the concentration of  $\text{Ag}^+$ , the development stages and deformities of embryos.

**Study of Concentration-Dependent Effects of  $\text{Ag}^+$  on the Hatching Timeline of Developing Embryos.** Zebrafish embryos hatch out of their chorions after organogenesis for survivability during 48–72 hpf. Individual embryos hatch sporadically during the whole third day of development and occasionally later. Thus, the timeline of hatching is not typically used as a staging index for the zebrafish development. Nonetheless, if the embryos stay inside the chorion for too long, it could lead to abnormal growth of embryos. During natural hatching, the chorion is digested from the inner surface by chorionolytic enzymes (e.g., chorionase) using a biochemical mechanism followed by mechanical mechanisms (e.g., tail movements) to further help the embryo to break the remaining chorion and free itself.<sup>51</sup> Studies have shown the delay in hatching after exposure to various toxins.<sup>52,53</sup> Mechanisms of the delay are not yet fully understood though the hardening of the outer layer of the chorion was assumed to make it difficult for the embryo to break free.

We studied the dependence of the hatching timeline of embryos on the  $\text{Ag}^+$  concentration and embryonic developmental deformity. The results in Figure 5A show that majority of normally developing embryos hatched by 66 hpf as embryos were chronically exposed to a lower concentration of  $\text{Ag}^+$  (0.05–0.1  $\mu\text{M}$ ), which are similar to those in the absence of  $\text{Ag}^+$  (the control experiment). As the concentration of  $\text{Ag}^+$  increases to 0.2 and 0.3  $\mu\text{M}$ , a substantial number of embryos hatched by 76 hpf. Interestingly, embryos with various hatching times during 46–96 hpf were observed as the embryos were chronically exposed to 0.2  $\mu\text{M}$   $\text{Ag}^+$  over 120 h, suggesting that individual embryos possess various distinctive responses to the toxic effects of  $\text{Ag}^+$  on embryonic development. As the concentration increases to 0.3  $\mu\text{M}$  and beyond, the number of embryos that became dead and deformed increases drastically, and normally developing embryos hatched during 46–76 hpf, suggesting that those embryos that did not hatch by 76 hpf could be dead or developed abnormally. Notably, as the concentration increases further to 0.4  $\mu\text{M}$ , the majority (67%) of normally developing embryos hatched during 46–56 hpf, 16% of them hatched during 67–76 hpf, while 17% of them did not hatch by 120 hpf. As the concentration increases to 0.8  $\mu\text{M}$ , none of embryos hatched before 66 hpf, and all normally developing embryos hatched at 67–76 hpf.

The abnormally developing embryos were observed after they were chronically treated with  $\text{Ag}^+$  (0.10–1.20  $\mu\text{M}$ ) for 120 hpf. A substantial number of the abnormally developing

embryos did not hatch, as shown in Figure 5B, which might be attributed to a delay in chemical release of hatching enzymes (e.g., chorionase) to digest the chorion and a lack of physical strength to move and break free out of the chorion due to deformities. As the concentration of  $\text{Ag}^+$  increases to 0.3  $\mu\text{M}$ , 75% of abnormally developing embryos show various hatching times (46–96 hpf), and 25% of them did not hatch by 120 hpf. Taken together, the result in Figure 5 shows that the hatching timeline of developing embryos highly depends upon the  $\text{Ag}^+$  concentration, and the concentration-dependent embryonic hatching timelines are not linear. The result suggests that multiple factors might affect the hatching timeline of developing embryos, and concentration-dependent abnormalities of developing embryos (Figures 2 and 3 and Table 1) could cause the delay of hatching or the inability to hatch.

**New Findings in Comparison of This Study with Our Previous Studies of Ag NPs.** The experiments in this study were conducted using the same approaches and the same conditions as those used in our previous studies of effects of Ag NPs on embryonic development of embryos,<sup>4–6,16,34,35</sup> which enables the comparison of findings from the study of effects of  $\text{Ag}^+$  on embryonic development with those of Ag NPs. In the presence of egg water (zebrafish embryonic medium, 1 mM NaCl), the highest concentration of free  $\text{Ag}^+$  is 0.18  $\mu\text{M}$  (19.4  $\mu\text{g}/\text{L}$ ) since the solubility product constant ( $K_{\text{sp}}$ ) of AgCl at 25 °C is  $1.80 \times 10^{-10}$ . The presence of  $\text{Ag}^+$  concentration higher than 0.18  $\mu\text{M}$  would lead to the generation of AgCl colloid NPs. The results from this study show that only 51% of cleavage-stage embryos (2 hpf) developed normally after being chronically treated with 0.25  $\mu\text{M}$   $\text{Ag}^+$  until 120 hpf, indicating a critical concentration of  $\text{Ag}^+$  at 0.25  $\mu\text{M}$ , which is higher than the solubility of  $\text{Ag}^+$  0.18  $\mu\text{M}$  in egg water. We observed only one or two abnormally developed embryos out of 36 embryos that were chronically treated with a given concentration of  $\text{Ag}^+$  (0.1 or 0.2  $\mu\text{M}$ ) until 120 hpf (Table 1). As the concentration of  $\text{Ag}^+$  increases, the number of embryos that became dead increases with the concentration. All embryos either became dead or developed abnormally after being chronically treated with 0.8  $\mu\text{M}$   $\text{Ag}^+$  or higher until 120 hpf.

Our previous studies show that ~50% of cleavage-stage embryos developed normally after being chronically treated with 80, 50, and 3.5 pM of 11.6  $\pm$  3.5, 41.6  $\pm$  9.1, and 97  $\pm$  13 nm Ag NPs until 120 hpf, respectively.<sup>4–7,16,33–35</sup> The solubility of  $\text{Ag}^+$  is 0.18  $\mu\text{M}$  (19.4  $\mu\text{g}/\text{L}$ ) in the presence of egg water (1 mM NaCl). If 4%, 0.16%, or 0.18% of 80, 50, and 3.5 pM of 11.6  $\pm$  3.5, 41.6  $\pm$  9.1, and 97  $\pm$  13 nm Ag NPs were released as  $\text{Ag}^+$ , it would generate 0.18  $\mu\text{M}$   $\text{Ag}^+$ , respectively. However, the embryos treated with Ag NPs until 120 hpf developed to larvae with much more severe deformities than those treated with  $\text{Ag}^+$ , and some of the deformities (e.g., severe cardiac malformation and no head) were only observed in the embryos treated with Ag NPs but not  $\text{Ag}^+$ . Furthermore, our previous studies show that the effects of Ag NPs on embryonic development highly depend upon the sizes of Ag NPs, and the large Ag NPs created more severe effects on embryonic development than small NPs, which further demonstrates that the effects of Ag NPs on embryonic development are attributed to the NPs themselves and their unique physicochemical properties but not the release of  $\text{Ag}^+$ .<sup>6,34</sup>

As we described in our previous studies,<sup>4–7,16,33–35</sup> the molar concentration of single Ag NPs (but not Ag atoms or ions) was used to study the concentration-dependent effect of

Ag NPs on embryonic development. Like distinctive molecules, differently sized Ag NPs have their distinctive NP (molecular) weights and physicochemical properties (e.g., surface area, reactivity, size, weight, and optical properties). Therefore, the molar concentration of the NPs (moles of NPs divided by the solution volume) is proportional to the number of single NPs and their surface areas. Unlike conventional chemicals, the weight/volume (w/v) of the Ag atom is not proportional to the surface properties and number (doses) of Ag NPs. Thus, the Ag NPs should not be described by the same atomic weight of Ag or w/v of the Ag atom or ions but the molar concentration of Ag NPs.

Furthermore, in our previous studies, we did not observe the release of Ag<sup>+</sup> from Ag NPs because LSPR spectra of single Ag NPs remained unchanged over 120 h of their incubation with egg water.<sup>4–7,16,33–35</sup> If the Ag<sup>+</sup> were released from Ag NPs, the size and shape of single NPs would have changed, which would have led to the shift of LSPR spectra of single NPs. Yet, other studies continue reporting and assuming that the effects of Ag NPs on the embryonic development were attributed to the release of Ag<sup>+</sup> from the Ag NPs.<sup>21,36–38</sup> Many of these studies were carried out using capped or unpurified Ag NPs, without careful characterization of single Ag NPs *in situ* and without control experiments.<sup>21,39–43</sup>

## SUMMARY

In summary, we have studied the concentration- and time-dependent effects of Ag<sup>+</sup> on embryonic development of zebrafish by chronically exposing cleavage-stage embryos (~2 hpf) with various concentrations of Ag<sup>+</sup> (0–1.2  $\mu$ M) in egg water (embryonic medium, 1 mM NaCl) until 120 hpf and imaging the morphological development, heart beats, and hatching of individual embryos over time. The results show that the effects of Ag<sup>+</sup> on embryonic development highly depend upon the concentration of Ag<sup>+</sup> and exposure time. As the concentration increases, the number of embryos that developed normally decreases, showing the critical concentration of Ag<sup>+</sup> at 0.25  $\mu$ M, where ~50% of embryos developed normally. As the concentration of Ag<sup>+</sup> increases from 0.05 to 0.3  $\mu$ M, the number of embryos that developed abnormally and became dead increases, and severity of deformities increases. As the concentration of Ag<sup>+</sup> increases further from 0.3 to 1.2  $\mu$ M, the embryos that became dead increases drastically, while the number of embryos that developed abnormally decreases. The effect of Ag<sup>+</sup> on embryonic development increases as the exposure time of embryos to Ag<sup>+</sup> increases and plateaus at 72 hpf. The results also show concentration-dependent effects on heart rates and hatching rates of developing embryos, primarily attributing to the concentration-dependent abnormally developing embryos. In comparison with our previous studies of the effects of Ag NPs on embryonic development, the results show that the toxic effects of Ag<sup>+</sup> on embryonic development significantly differ from those of Ag NPs, and the toxic effects of Ag<sup>+</sup> on embryonic development are far less severe than Ag NPs, which further demonstrates that toxic effects of Ag NPs on embryonic development are not attributed to the releasing of Ag<sup>+</sup> from Ag NPs but Ag NPs themselves and their unique physicochemical properties.

## AUTHOR INFORMATION

### Corresponding Author

Xiao-Hong Nancy Xu – Department of Chemistry and Biochemistry & Department of Electrical and Computer Engineering (Biomedical Engineering), Old Dominion University, Norfolk, Virginia 23529, United States; [orcid.org/0000-0002-7470-1948](https://orcid.org/0000-0002-7470-1948); Email: [xhxu@odu.edu](mailto:xhxu@odu.edu); Fax: (757) 683-5698

### Authors

Martha S. Johnson – Department of Chemistry and Biochemistry & Department of Electrical and Computer Engineering (Biomedical Engineering), Old Dominion University, Norfolk, Virginia 23529, United States; [orcid.org/0000-0002-0476-5567](https://orcid.org/0000-0002-0476-5567)

Preeyaporn Songkiatisak – Department of Chemistry and Biochemistry & Department of Electrical and Computer Engineering (Biomedical Engineering), Old Dominion University, Norfolk, Virginia 23529, United States; [orcid.org/0000-0002-0205-4673](https://orcid.org/0000-0002-0205-4673)

Pavan Kumar Cherukuri – Department of Chemistry and Biochemistry & Department of Electrical and Computer Engineering (Biomedical Engineering), Old Dominion University, Norfolk, Virginia 23529, United States; [orcid.org/0000-0001-9384-9166](https://orcid.org/0000-0001-9384-9166)

Complete contact information is available at:

<https://pubs.acs.org/10.1021/acsomega.2c05504>

### Notes

The authors declare no competing financial interest.

## ACKNOWLEDGMENTS

This work was supported in part by NSF (NIRT-CBET 0507036 and CBET 1450936) and NIH (R01GM0764401, R15GM119116, R21HL127580, and R21GM141780). M.S.J. is grateful for support of NSF-GRDS (CBET 1450936). We would like to thank Lauren Browning for her participation and assistance in the preliminary study of this work.

## REFERENCES

- (1) Cunningham, B.; Engstrom, A. M.; Harper, B. J.; Harper, S. L.; Mackiewicz, M. R. Silver Nanoparticles Stable to Oxidation and Silver Ion Release Show Size-Dependent Toxicity In Vivo. *Nanomaterials* **2021**, *11*, 1516.
- (2) Wang, T.; Liu, W. Emerging investigator series: metal nanoparticles in freshwater: transformation, bioavailability and effects on invertebrates. *Environ. Sci. Nano.* **2022**, *9*, 2237–2263.
- (3) Lubick, N. Nanosilver toxicity: ions, nanoparticles—or both? *Environ. Sci. Technol.* **2008**, *42*, 8617.
- (4) Lee, K. J.; Browning, L. M.; Nallathamby, P. D.; Osgood, C. J.; Xu, X. H. N. In vivo imaging of transport and biocompatibility of single silver nanoparticles in early development of zebrafish embryos. *ACS Nano* **2007**, *1*, 133–143.
- (5) Lee, K. J.; Browning, L. M.; Nallathamby, P. D.; Xu, X.-H. N. Silver nanoparticles induce developmental stage-specific embryonic phenotypes in zebrafish. *Nanoscale* **2013**, *5*, 11625–11636.
- (6) Lee, K. J.; Browning, L. M.; Nallathamby, P. D.; Desai, T.; Cherukuri, P. K.; Xu, X.-H. N. In vivo quantitative study of size-dependent transport and toxicity of single silver nanoparticles using zebrafish embryos. *Chem. Res. Toxicol.* **2012**, *25*, 1029–1046.
- (7) Browning, L. M.; Lee, K. J.; Huang, T.; Nallathamby, P. D.; Lowman, J.; Xu, X. H. N. Random walk of single gold nanoparticles in zebrafish embryos leading to stochastic toxic effects on embryonic developments. *Nanoscale* **2009**, *1*, 138–152.



- (8) Kazemzadeh-Narbat, M.; Cheng, H.; Chabok, R.; Alvarez, M. M.; De La Fuente-Nunez, C.; Phillips, K. S.; Khademhosseini, A. Strategies for antimicrobial peptide coatings on medical devices: A review and regulatory science perspective. *Crit. Rev. Biotechnol.* **2021**, *41*, 94–120.
- (9) Kyriacou, S. V. *Real-time study of multidrug resistance mechanism in Pseudomonas aeruginosa using nanoparticle optics and single live cell imaging*. Old Dominion University: Norfolk, VA, 2003.
- (10) Songkiatisak, P.; Ding, F.; Cherukuri, P. K.; Xu, X.-H. N. Size-dependent inhibitory effects of antibiotic nanocarriers on filamentation of *E. coli*. *Nanoscale Adv.* **2020**, *2*, 2135–2145.
- (11) Xu, X.-H. N.; Chen, J.; Jeffers, R. B.; Kyriacou, S. Direct measurement of sizes and dynamics of single living membrane transporters using nano-optics. *Nano Lett.* **2002**, *2*, 175–182.
- (12) EPA. *National Recommended Water Quality Criteria Tables*. <https://www.epa.gov/wqc/national-recommended-water-quality-criteria-tables>.
- (13) Huang, T.; Xu, X.-H. N. Synthesis and characterization of tunable rainbow-colored silver nanoparticle solutions using single-nanoparticle plasmonic microscopy and spectroscopy. *J. Mater. Chem.* **2010**, *20*, 9867–9876.
- (14) Mie, G. Beitrag zur optik trüber medien, speziell kolloidaler metrallosungen. *Annu. Phys.* **1908**, *25*, 377–445.
- (15) Nallathamby, P. D.; Huang, T.; Xu, X.-H. N. Design and characterization of optical nanorulers of single nanoparticles using optical microscopy and spectroscopy. *Nanoscale* **2010**, *2*, 1715–1722.
- (16) Lee, K. J.; Browning, L. M.; Nallathamby, P. D.; Xu, X. H. N. Study of charge-dependent transport and toxicity of peptide-functionalized silver nanoparticles using zebrafish embryos and single nanoparticle plasmonic spectroscopy. *Chem. Res. Toxicol.* **2013**, *26*, 904–917.
- (17) Nallathamby, P. D.; Xu, X.-H. N. Study of cytotoxic and therapeutic effects of stable and purified silver nanoparticles on tumor cells. *Nanoscale* **2010**, *2*, 942–952.
- (18) Terzioğlu, E.; Arslan, M.; Balaban, B.; Çakar, Z. Microbial silver resistance mechanisms: recent developments. *World J. Microbiol. Biotechnol.* **2022**, *38*, 158.
- (19) Xu, X.-H. N.; Kyriacou, S.; Jeffers, R. Metallic Nanoparticles for Inhibition of Bacterium Growth. US Patent App. 10/484.485 2003.
- (20) Istiqola, A.; Syafiuddin, A. A review of silver nanoparticles in food packaging technologies: Regulation, methods, properties, migration, and future challenges. *Chin. Chem. Soc.* **2020**, *67*, 1942–1956.
- (21) Nowack, B.; Krug, H. F.; Height, M. 120 years of nanosilver history: implications for policy makers. *Environ. Sci. Technol.* **2011**, *45*, 1177–1183.
- (22) Nallathamby, P. D.; Lee, K. J.; Desai, T.; Xu, X.-H. N. Study of multidrug membrane transporters of single living pseudomonas aeruginosa cells using size-dependent plasmonic nanoparticle optical probes. *Biochemistry* **2010**, *49*, 5942–5953.
- (23) Nallathamby, P. D.; Lee, K. J.; Xu, X.-H. N. Design of stable and uniform single nanoparticle photonics for in vivo dynamics imaging of nanoenvironments of zebrafish embryonic fluids. *ACS Nano* **2008**, *2*, 1371–1380.
- (24) Huang, T.; Browning, L. M.; Xu, X.-H. N. Far-field photostable optical nanoscopy (PHOTON) for real-time super-resolution single-molecular imaging of signaling pathways of single live cells. *Nanoscale* **2012**, *4*, 2797–2812.
- (25) Huang, T.; Nallathamby, P. D.; Gillet, D.; Xu, X.-H. N. Design and synthesis of single nanoparticle optical biosensors for imaging and characterization of single receptor molecules on single living cells. *Anal. Chem.* **2007**, *79*, 7708–7718.
- (26) Huang, T.; Nallathamby, P. D.; Xu, X.-H. N. Photostable single-molecule nanoparticle optical biosensors for real-time sensing of single cytokine molecules and their binding reactions. *J. Am. Chem. Soc.* **2008**, *130*, 17095–17105.
- (27) Huang, T.; Xu, X. H. N. Multicolored nanometer-resolution mapping of single protein-ligand binding complex using far-field photostable optical nanoscopy (PHOTON). *Nanoscale* **2011**, *3*, 3567–3572.
- (28) Kyriacou, S. V.; Brownlow, W. J.; Xu, X. H. N. Using nanoparticle optics assay for direct observation of the function of antimicrobial agents in single live bacterial cells. *Biochemistry* **2004**, *43*, 140–147.
- (29) Xu, X. H. N. Far-Field Photostable Optical Nanoscopy (PHOTON). In *Encyclopedia of Spectroscopy and Spectrometry (Third Edition)*, Lindon, J., Tranter, G. E., Koppenaal, D. Eds.; Vol. 1; Elsevier, 2017; pp. 566–570.
- (30) Xu, X.-H. N.; Brownlow, W. J.; Kyriacou, S. V.; Wan, Q.; Viola, J. J. Real-time probing of membrane transport in living microbial cells using single nanoparticle optics and living cell imaging. *Biochemistry* **2004**, *43*, 10400–10413.
- (31) Cherukuri, P. K.; Songkiatisak, P.; Ding, F.; Jault, J.-M.; Xu, X.-H. N. Antibiotic Drug Nanocarriers for Probing of Multidrug ABC Membrane Transporter of *Bacillus subtilis*. *ACS Omega* **2020**, *5*, 1625–1633.
- (32) Ding, F.; Songkiatisak, P.; Cherukuri, P. K.; Huang, T.; Xu, X.-H. N. Size-Dependent Inhibitory Effects of Antibiotic Drug Nanocarriers against *Pseudomonas aeruginosa*. *ACS Omega* **2018**, *3*, 1231–1243.
- (33) Browning, L. M.; Huang, T.; Xu, X.-H. N. Real-time in vivo imaging of size-dependent transport and toxicity of gold nanoparticles in zebrafish embryos using single nanoparticle plasmonic spectroscopy. *Interface Focus* **2013**, *3*, 20120098.
- (34) Browning, L. M.; Lee, K. J.; Nallathamby, P. D.; Xu, X.-H. N. Silver nanoparticles incite size and dose-dependent developmental phenotypes and nanotoxicity in zebrafish embryos. *Chem. Res. Toxicol.* **2013**, *26*, 1503–1513.
- (35) Lee, K. J.; Nallathamby, P. D.; Browning, L. M.; Desai, T.; Cherukuri, P.; Xu, X.-H. N. Single nanoparticle spectroscopy for real-time in vivo quantitative analysis of transport and toxicity of single nanoparticles in single embryos. *Analyst* **2012**, *137*, 2973–2986.
- (36) Fabrega, J.; Luoma, S. N.; Tyler, C. R.; Galloway, T. S.; Lead, J. R. Silver nanoparticles: Behaviour and effects in the aquatic environment. *Environ. Int.* **2011**, *37*, 517–531.
- (37) van Aerle, R.; Lange, A.; Moorhouse, A.; Paszkiewicz, K.; Ball, K.; Johnston, B. D.; de-Bastos, E.; Booth, T.; Tyler, C. R.; Santos, E. M. Molecular mechanisms of toxicity of silver nanoparticles in zebrafish embryos. *Environ. Sci. Technol.* **2013**, *47*, 8005–8014.
- (38) Groh, K. J.; Dalkvist, T.; Piccapietra, F.; Behra, R.; Suter, M. J.-F.; Schirmer, K. Critical influence of chloride ions on silver ion-mediated acute toxicity of silver nanoparticles to zebrafish embryos. *Nanotoxicology* **2015**, *9*, 81–91.
- (39) Olasagasti, M.; Gatti, A. M.; Capitani, F.; Barranco, A.; Pardo, M. A.; Escuredo, K.; Rainieri, S. Toxic effects of colloidal nanosilver in zebrafish embryos. *J. Appl. Toxicol.* **2014**, *34*, 562–575.
- (40) Gao, J.; Mahapatra, C. T.; Mapes, C. D.; Khlebnikova, M.; Wei, A.; Sepúlveda, M. S. Vascular toxicity of silver nanoparticles to developing zebrafish (*Danio rerio*). *Nanotoxicology* **2016**, *10*, 1363–1372.
- (41) Cui, B.; Ren, L.; Xu, Q.-H.; Yin, L.-Y.; Zhou, X.-Y.; Liu, J.-X. Silver nanoparticles inhibited erythropoiesis during zebrafish embryogenesis. *Aquat. Toxicol.* **2016**, *177*, 295–305.
- (42) Caloudova, H.; Hodkovicova, N.; Sehonova, P.; Blahova, J.; Marsalek, B.; Panacek, A.; Svobodova, Z. The effect of silver nanoparticles and silver ions on zebrafish embryos (*Danio rerio*). *Neuroendocrinol. Lett.* **2018**, *39*, 299–304.
- (43) Jemec, A.; Kahru, A.; Potthoff, A.; Drobne, D.; Heinlaan, M.; Böhme, S.; Geppert, M.; Novak, S.; Schirmer, K.; Rekulapally, R.; Singh, S.; Aruoja, V.; Sihtmäe, M.; Juganson, K.; Käkinen, A.; Kühnel, D. An interlaboratory comparison of nanosilver characterization and hazard identification: Harmonising techniques for high quality data. *Environ. Int.* **2016**, *87*, 20–32.
- (44) Kahn, P. Zebrafish hit the big time. *Science* **1994**, *264*, 904–905.
- (45) Lieschke, G. J.; Currie, P. D. Animal models of human disease: zebrafish swim into view. *Nat. Rev. Genet.* **2007**, *8*, 353–367.

(46) Peterson, R. T.; Macrae, C. A. Systematic approaches to toxicology in the zebrafish. *Annu. Rev. Pharmacol. Toxicol.* **2012**, *52*, 433–453.

(47) Hill, A. J.; Teraoka, H.; Heideman, W.; Peterson, R. E. Zebrafish as a model vertebrate for investigating chemical toxicity. *Toxicol. Sci.* **2005**, *86*, 6–19.

(48) Howe, K.; Clark, M. D.; Torroja, C. F.; Torrance, J.; Berthelot, C.; Muffato, M.; Collins, J. E.; Humphray, S.; McLaren, K.; Matthews, L.; McLaren, S.; Sealy, I.; Caccamo, M.; Churcher, C.; Scott, C.; Barrett, J. C.; Koch, R.; Rauch, G. J.; White, S.; Chow, W.; Kilian, B.; Quintais, L. T.; Guerra-Assunção, J. A.; Zhou, Y.; Gu, Y.; Yen, J.; Vogel, J. H.; Eyre, T.; Redmond, S.; Banerjee, R.; Chi, J.; Fu, B.; Langle, E.; Maguire, S. F.; Laird, G. K.; Lloyd, D.; Kenyon, E.; Donaldson, S.; Sehra, H.; Almeida-King, J.; Loveland, J.; Trevanion, S.; Jones, M.; Quail, M.; Willey, D.; Hunt, A.; Burton, J.; Sims, S.; McLay, K.; Plumb, B.; Davis, J.; Clee, C.; Oliver, K.; Clark, R.; Riddle, C.; Elliott, D.; Threadgold, G.; Harden, G.; Ware, D.; Begum, S.; Mortimore, B.; Kerry, G.; Heath, P.; Phillimore, B.; Tracey, A.; Corby, N.; Dunn, M.; Johnson, C.; Wood, J.; Clark, S.; Pelan, S.; Griffiths, G.; Smith, M.; Glithero, R.; Howden, P.; Barker, N.; Lloyd, C.; Stevens, C.; Harley, J.; Holt, K.; Panagiotidis, G.; Lovell, J.; Beasley, H.; Henderson, C.; Gordon, D.; Auger, K.; Wright, D.; Collins, J.; Raisen, C.; Dyer, L.; Leung, K.; Robertson, L.; Ambridge, K.; Leongamornlert, D.; McGuire, S.; Gilderthorp, R.; Griffiths, C.; Manthavadi, D.; Nichol, S.; Barker, G.; Whitehead, S.; Kay, M.; Brown, J.; Murnane, C.; Gray, E.; Humphries, M.; Sycamore, N.; Barker, D.; Saunders, D.; Wallis, J.; Babbage, A.; Hammond, S.; Mashreghi-Mohammadi, M.; Barr, L.; Martin, S.; Wray, P.; Ellington, A.; Matthews, N.; Ellwood, M.; Woodmansey, R.; Clark, G.; Cooper, J. D.; Tromans, A.; Grafham, D.; Skuce, C.; Pandian, R.; Andrews, R.; Harrison, E.; Kimberley, A.; Garnett, J.; Fosker, N.; Hall, R.; Garner, P.; Kelly, D.; Bird, C.; Palmer, S.; Gehring, I.; Berger, A.; Dooley, C. M.; Ersan-Urün, Z.; Eser, C.; Geiger, H.; Geisler, M.; Karotki, L.; Kirn, A.; Konantz, J.; Konantz, M.; Oberländer, M.; Rudolph-Geiger, S.; Teucke, M.; Lanz, C.; Raddatz, G.; Osoegawa, K.; Zhu, B.; Rapp, A.; Widaa, S.; Langford, C.; Yang, F.; Schuster, S. C.; Carter, N. P.; Harrow, J.; Ning, Z.; Herrero, J.; Searle, S. M. J.; Enright, A.; Geisler, R.; Plasterk, R. H. A.; Lee, C.; Westerfield, M.; de Jong, P. J.; Zon, L. I.; Postlethwait, J. H.; Nüsslein-Volhard, C.; Hubbard, T. J. P.; Crollius, H. R.; Rogers, J.; Stemple, D. L. The zebrafish reference genome sequence and its relationship to the human genome. *Nature* **2013**, *496*, 498–503.

(49) Woods, I. G.; Wilson, C.; Friedlander, B.; Chang, P.; Reyes, D. K.; Nix, R.; Kelly, P. D.; Chu, F.; Postlethwait, J. H.; Talbot, W. S. The zebrafish gene map defines ancestral vertebrate chromosomes. *Genome Res.* **2005**, *15*, 1307–1314.

(50) Zon, L. I.; Peterson, R. T. In vivo drug discovery in the zebrafish. *Nat. Rev. Drug Discovery* **2005**, *4*, 35–44.

(51) Helvik, J. V.; Walther, B. T. Photoregulation of the hatching process of halibut (*Hippoglossus hippoglossus*) eggs. *J. Exp. Zool.* **1992**, *263*, 204–209.

(52) Pompermaier, A.; Varela, A.; Mozzato, M.; Soares, S.; Fortuna, M.; Alves, C.; Tamagno, W.; Barcellos, L. Impaired initial development and behavior in zebrafish exposed to environmentally relevant concentrations of widely used pesticides. *Comp. Biochem. Physiol., Part C: Toxicol. Pharmacol.* **2022**, *257*, No. 109328.

(53) Juan-García, A.; Bind, M.-A.; Engert, F. Larval zebrafish as an in vitro model for evaluating toxicological effects of mycotoxins. *Ecotoxicol. Environ. Saf.* **2020**, *202*, No. 110909.